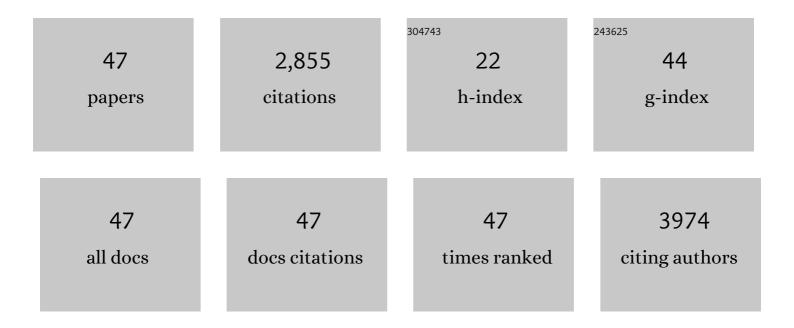
Zhi-qiang Wang

List of Publications by Year in descending order

Source: https://exaly.com/author-pdf/7481712/publications.pdf Version: 2024-02-01



#	Article	IF	CITATIONS
1	Dopant-induced electron localization drives CO2 reduction to C2 hydrocarbons. Nature Chemistry, 2018, 10, 974-980.	13.6	781
2	Atomic layer deposited Pt-Ru dual-metal dimers and identifying their active sites for hydrogen evolution reaction. Nature Communications, 2019, 10, 4936.	12.8	371
3	Boosting CO ₂ Electroreduction to CH ₄ via Tuning Neighboring Single-Copper Sites. ACS Energy Letters, 2020, 5, 1044-1053.	17.4	326
4	Double sulfur vacancies by lithium tuning enhance CO2 electroreduction to n-propanol. Nature Communications, 2021, 12, 1580.	12.8	162
5	High loading single-atom Cu dispersed on graphene for efficient oxygen reduction reaction. Nano Energy, 2019, 66, 104088.	16.0	138
6	Quantum-Dot-Derived Catalysts for CO2 Reduction Reaction. Joule, 2019, 3, 1703-1718.	24.0	106
7	Substrate strain tunes operando geometric distortion and oxygen reduction activity of CuN2C2 single-atom sites. Nature Communications, 2021, 12, 6335.	12.8	95
8	Zeroâ€Thermal Quenching of Mn ²⁺ Red Luminescence via Efficient Energy Transfer from Eu ²⁺ in BaMgP ₂ O ₇ . Advanced Optical Materials, 2019, 7, 1901187.	7.3	89
9	Electron Localization and Lattice Strain Induced by Surface Lithium Doping Enable Ampere‣evel Electrosynthesis of Formate from CO ₂ . Angewandte Chemie - International Edition, 2021, 60, 25741-25745.	13.8	66
10	BiVO4 nano–leaves: Mild synthesis and improved photocatalytic activity for O2 production under visible light irradiation. CrystEngComm, 2011, 13, 2500.	2.6	65
11	Six-Fold-Symmetrical Hierarchical ZnO Nanostructure Arrays: Synthesis, Characterization, and Field Emission Properties. Crystal Growth and Design, 2010, 10, 2455-2459.	3.0	61
12	Facile synthesis of anatase TiO2 mesocrystal sheets with dominant {001} facets based on topochemical conversion. CrystEngComm, 2010, 12, 3425.	2.6	54
13	Epitaxial Growth of ZnO Nanowires on ZnS Nanobelts by Metal Organic Chemical Vapor Deposition. Crystal Growth and Design, 2008, 8, 3911-3913.	3.0	46
14	Electronic behaviour of Au-Pt alloys and the 4f binding energy shift anomaly in Au bimetallics- X-ray spectroscopy studies. AIP Advances, 2018, 8, .	1.3	41
15	Tracking the Interface of an Individual ZnS/ZnO Nano-Heterostructure. Journal of Physical Chemistry C, 2012, 116, 10375-10381.	3.1	33
16	Selective atomic layer deposition of RuO _x catalysts on shape-controlled Pd nanocrystals with significantly enhanced hydrogen evolution activity. Journal of Materials Chemistry A, 2018, 6, 24397-24406.	10.3	31
17	Will Fluoride Toughen or Weaken Our Teeth? Understandings Based on Nucleation, Morphology, and Structural Assembly. Journal of Physical Chemistry B, 2009, 113, 16393-16399.	2.6	30
18	Elucidating the Many-Body Effect and Anomalous Pt and Ni Core Level Shifts in X-ray Photoelectron Spectroscopy of Pt–Ni Alloys. Journal of Physical Chemistry C, 2020, 124, 2313-2318.	3.1	29

ZHI-QIANG WANG

#	Article	IF	CITATIONS
19	Origin of luminescence from ZnO/CdS core/shell nanowire arrays. Nanoscale, 2014, 6, 9783-9790.	5.6	27
20	Highlyâ€Exposed Singleâ€Interlayered Cu Edges Enable Highâ€Rate CO ₂ â€toâ€CH ₄ Electrosynthesis. Advanced Energy Materials, 2022, 12, .	19.5	26
21	Unfolding the Anatase-to-Rutile Phase Transition in TiO ₂ Nanotubes Using X-ray Spectroscopy and Spectromicroscopy. Journal of Physical Chemistry C, 2016, 120, 22079-22087.	3.1	23
22	Probing defect emissions in bulk, micro- and nano-sized α-Al2O3 via X-ray excited optical luminescence. Journal of Chemical Physics, 2013, 138, 084706.	3.0	22
23	MnO2 nanolayers on highly conductive TiO0.54N0.46 nanotubes for supercapacitor electrodes with high power density and cyclic stability. Physical Chemistry Chemical Physics, 2014, 16, 8521.	2.8	21
24	Nanoscale Clarification of the Electronic Structure and Optical Properties of TiO ₂ Nanowire with an Impurity Phase upon Sodium Intercalation. Journal of Physical Chemistry C, 2015, 119, 17848-17856.	3.1	21
25	2D XANES-XEOL mapping: observation of enhanced band gap emission from ZnO nanowire arrays. Nanoscale, 2014, 6, 6531-6536.	5.6	20
26	Electron Localization and Lattice Strain Induced by Surface Lithium Doping Enable Ampere‣evel Electrosynthesis of Formate from CO ₂ . Angewandte Chemie, 2021, 133, 25945-25949.	2.0	19
27	Structure and optical properties of individual hierarchical ZnS nanobelt/ZnO nanorod heterostructures. CrystEngComm, 2011, 13, 6774.	2.6	14
28	Synthesis, characterization and optical properties of ZnS nanobelt/ZnO nanoparticle heterostructures. Materials Letters, 2012, 82, 29-32.	2.6	14
29	Effect of oxidation state of manganese in manganese oxide thin films on their capacitance performances. Surface Science, 2018, 676, 71-76.	1.9	13
30	Antimonyâ€Functionalized Phosphineâ€Based Photopolymer Networks. Angewandte Chemie - International Edition, 2018, 57, 13252-13256.	13.8	13
31	Lithium Vacancyâ€Tuned [CuO ₄] Sites for Selective CO ₂ Electroreduction to C ₂₊ Products. Small, 2022, 18, e2106433.	10.0	13
32	lmaging of drug loading distributions in individual microspheres of calcium silicate hydrate – an X-ray spectromicroscopy study. Nanoscale, 2015, 7, 6767-6773.	5.6	11
33	Tracking Drug Loading Capacities of Calcium Silicate Hydrate Carrier: A Comparative X-ray Absorption Near Edge Structures Study. Journal of Physical Chemistry B, 2015, 119, 10052-10059.	2.6	10
34	Tracking the transformations of mesoporous microspheres of calcium silicate hydrate at the nanoscale upon ibuprofen release: a XANES and STXM study. CrystEngComm, 2015, 17, 4117-4124.	2.6	8
35	Scanning transmission X-ray microscopy studies of chromium hydroxide hollow spheres and nanoparticles formed by gamma radiation. Canadian Journal of Chemistry, 2017, 95, 1146-1150.	1.1	8
36	Strain and ligand effects in Pt-Ni alloys studied by valence-to-core X-ray emission spectroscopy. Scientific Reports, 2021, 11, 13698.	3.3	7

ZHI-QIANG WANG

#	Article	IF	CITATIONS
37	Tip-Enhanced Raman Spectroscopy and Tip-Enhanced Photoluminescence of MoS ₂ Flakes Decorated with Gold Nanoparticles. Journal of Physical Chemistry C, 0, , .	3.1	7
38	Antimonyâ€Functionalized Phosphineâ€Based Photopolymer Networks. Angewandte Chemie, 2018, 130, 13436-13440.	2.0	6
39	High Energy Resolution Fluorescence Detection of the Pt L _{3,2} -Edge Whitelines of Pt-Based Bimetallic Systems: Implications for the Pt 5d _{5/2,3/2} Density of States. Journal of Physical Chemistry C, 2021, 125, 2327-2333.	3.1	6
40	Investigation of luminescence mechanism in La0.2Y1.8O3 scintillator. Journal of Luminescence, 2016, 173, 99-104.	3.1	5
41	Tracking the interaction of drug molecules with individual mesoporous amorphous calcium phosphate/ATP nanocomposites – an X-ray spectromicroscopy study. Physical Chemistry Chemical Physics, 2020, 22, 13108-13117.	2.8	5
42	A Comprehensive Investigation of a Zwitterionic Ge ^I Dimer with a 1,2â€Dicationic Core. Chemistry - A European Journal, 2019, 25, 14790-14800.	3.3	4
43	TiO ₂ Nanotubes: Morphology, Size, Crystallinity, and Phase-Dependent Properties from Synchrotron-Spectroscopy Studies. Journal of Physical Chemistry C, 2022, 126, 3265-3275.	3.1	3
44	Investigation of amorphous to crystalline phase transition of sodium titanate by X-ray absorption spectroscopy and scanning transmission X-ray microscopy. Canadian Journal of Chemistry, 2017, 95, 1163-1169.	1.1	2
45	Imaging of Individual Eu Doped Y2O3 Sub-microspheres Using Photoluminescence Yield: An Application of Scanning Transmission X-ray Microscopy in Luminescent Materials. Microscopy and Microanalysis, 2018, 24, 480-481.	0.4	2
46	Polymer networks functionalized with <scp>lowâ€valent</scp> phosphorus cations. Journal of Polymer Science, 0, , .	3.8	1
47	Frontispiece: A Comprehensive Investigation of a Zwitterionic Ge ^I Dimer with a 1,2â€Dicationic Core. Chemistry - A European Journal, 2019, 25, .	3.3	0